MECHANICS AND CONTROL
Vol. 32 No. 2 2013 http://dx.doi.org/10.7494/mech.2013.32.2.82

Mateusz Wolnica*

MR DAMPER INVERSE MODELING DEPENDENT ON OPERATING CONDITIONS

SUMMARY

For semi-active control of vehicle suspension magnetoreological (MR) dampers are usually used. Construction of such dampers suggests that their properties should be dependent on fluid temperature, current of the coil and the relative velocity of the rod, which all change during operation. Then, an inverse model used to work out the current based on the required damping force may not be adequate, and performance of the overall semi-active control system can be significantly degraded. MR damper reaches its operating temperature in a short period of time, and thus it should be modelled, and the obtained inverse model should reflect such state. However, it has been observed that the hysteric behaviour of the MR damper significantly differs depending on the current. The paper presents results of such analysis and recommends using a set of simple models appropriate for different ranges of this parameter. During control the models should be switched to guarantee the best operating conditions. Experiments for this research have been performed using MTS system.

Keywords: *MR damper, inverse model, gain scheduling*

MODELOWANIE TŁUMIKA MR Z UWZGLĘDNIENIEM WARUNKÓW PRACY

W półaktywnym sterowaniu zawieszeniem pojazdu mogą być wykorzystane tłumiki magnetoreologiczne (MR). Z właściwości konstrukcji tłumika wynika, że na jego pracę może wpływać względna prędkość tłoczyska, natężenie prądu na cewce tłumika oraz temperatura cieczy MR. Każde z tych parametrów może ulegać zmianie w trakcie działania tłumika. Tłumik MR osiąga stałą temperaturę pracy w krótkim okresie czasu i dla takiej temperatury powinien być modelowany. Jednak zaobserwowano, że dla różnych wartości natężenia prądu na cewce tłumika charakterystyka tłumika zmienia się. W pracy przedstawiono wyniki opracowania kilku prostych modeli odwrotnych dla różnych zakresów natężenia prądu. W trakcie sterowania występuje przełączanie między poszczególnymi modelami odwrotnymi w zależności od warunków pracy. Dane eksperymentalne zebrano wykorzystując do badań tłumika maszynę wytrzymałościową.

Słowa kluczowe: *tłumik magnetoreologiczny, modelowanie odwrotne, harmonogramowanie wzmocnienia*

1. INTRODUCTION

For semi-active control of vehicle suspension magnetorheological (MR) dampers are usually used (Wang *et al.* 2011, Kamalakkannan *et al.* 2012, Krauze 2011, Wolnica *et al.* 2013, Kurczyk *et al.* 2013). Construction of such dampers suggests that their properties should depend on the current of the coil, the relative velocity of the rod and temperature of the fluid, which all change during operation. Then, an inverse model used to work out the current based on the required damping force may not be adequate, and performance of the overall semi-active control system can be significantly degraded. MR damper reaches its operating temperature in a short period of time, and thus it should be modelled, and the obtained inverse model should reflect such state. However, it has been observed that the hysteric behaviour of the MR damper significantly differs depending on the current. The paper presents results of such analysis and recommends using a set of simple models appropriate for different ranges of this parameter (Fialho *et al.* 2000). During control the models should be switched to guarantee the best operating conditions. Experiments for this research have been performed using a material testing system (MTS).

2. MR DAMPER MODELLING AND INVERSE MODELLING

In this paper, in order to capture the damper behaviour, a cascade of nonlinear hypertangent models is used (Bouc 1967, Guo *et al.* 2006, Sapiński 2009). Construction of an MR damper is shown in figure 1.

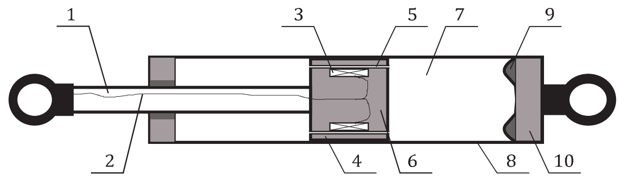

Fig. 1. The construction of MR damper: 1 – rod, 2 – coil power cables, 3 – coil, 4 – ring, 5 – annular gap, 6 – piston, 7 – MR fluid, 8 – cylinder, 9 – membrane, 10 – accumulator

In experiments the MR damper produced by LORD company (RD-8040-1) was used. Its properties are shown in the table 1.

* Division of Mechatronic Systems, Institute of Mining Technology KOMAG, Gliwice, Poland; mwolnica@komag.eu

Table 1

Properties of the RD-8040-1 MR damper

Parameter	Value
Stroke [mm]	55
Extended length [mm]	208
Tensile strength [N]	8896
Max. damper forces [N]	~2500
Operating temperature [ºC]	71
Input current [A]	Continuous: 1 Intermittent: 2
Input voltage [V]	12DC
Resistance [Ω]	Ambient temp.: 5 Max. operating temperature: 7

Experimental data were collected using material testing system MTS 858 Table Top System. During experiments the current was changed from 0 [A] to 1 [A] with the step of 0.1 [A]. The frequency and amplitude of the excitation were constant and set to 1 [Hz] and 25 [mm], respectively.

The force of the MR damper can be obtained as follows:

$$F_t = F_c \mathrm{tgh}(\alpha((\dot{x}-\dot{z}) + p_1(x-z))) + c_0((\dot{x}-\dot{z}) + p_2(x-z)) \tag{1}$$

where F_c and c_0 are dependent on the current i by first-degree polynomials. Terms $(\dot{x}-\dot{z})$ and $(x-z)$ are the relative displacement and the relative velocity of the rod, respectively. Parameters α, p_1, p_2 are constant, and they express properties of MR damper hysteric behaviours. To ensure that the model is invertible, first-degree polynomials can be used for F_c and c_0. Parameters do not have any physical meaning:

$$F_c = f_1 i + f_2, \quad c_0 = f_3 i + f_4 . \tag{2}$$

Then, the inverse MR damper model takes the form:

$$i = \frac{F_t - f_2 \mathrm{tgh}(\alpha((\dot{x}-\dot{z}) + p_1(x-z))) - f_4((\dot{x}-\dot{z}) + p_2(x-z))}{f_1 \mathrm{tgh}(\alpha((\dot{x}-\dot{z}) + p_1(x-z))) + f_3((\dot{x}-\dot{z}) + p_2(x-z))} . \tag{3}$$

3. INFLUENCE OF OPERATING CONDITIONS

A cascade of simple inverse models M_3 (see fig. 2) is proposed in this paper to be used instead of complicated models used in the literature.

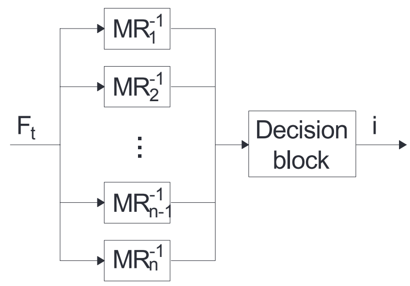

Fig. 2. A cascade of inverse MR damper models, further referred to as inverse models M_3

In the cascade, each inverse model is tuned for a narrow range of the current. Parameter F_c has the greatest influence on the final value of F_t. Its dependence on the coils current is shown in figure 3. Parameter c_0 depends on the current too, but its influence on the final value is small. Its dependence on the coils current is shown in figure 4.

The range of change is split to minimize the difference between experimental data values and model values. The MR_1^{-1} model is tuned for the current i in the range 0–0.1 [A], the MR_2^{-1} model is tuned for the current in the range 0.1–0.25 [A], etc.

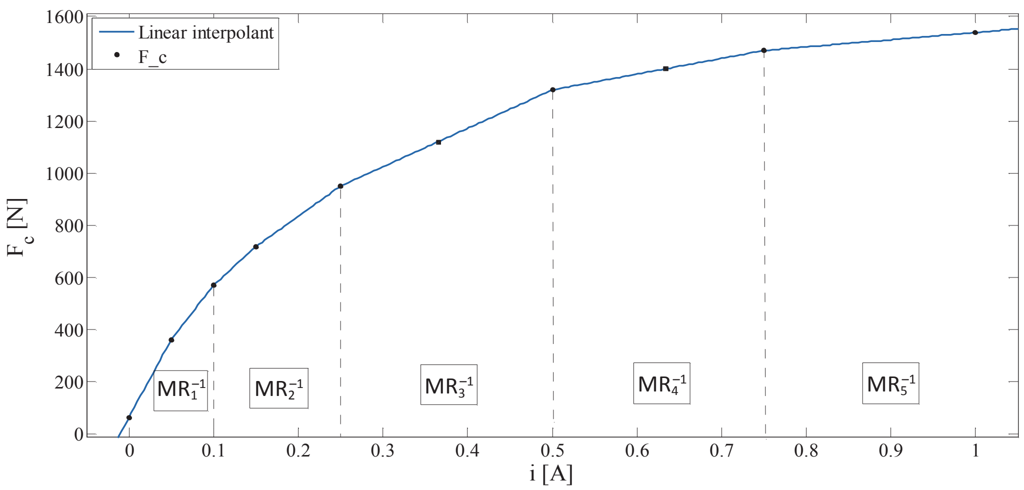

Fig. 3. The F_c parameter dependence on current i

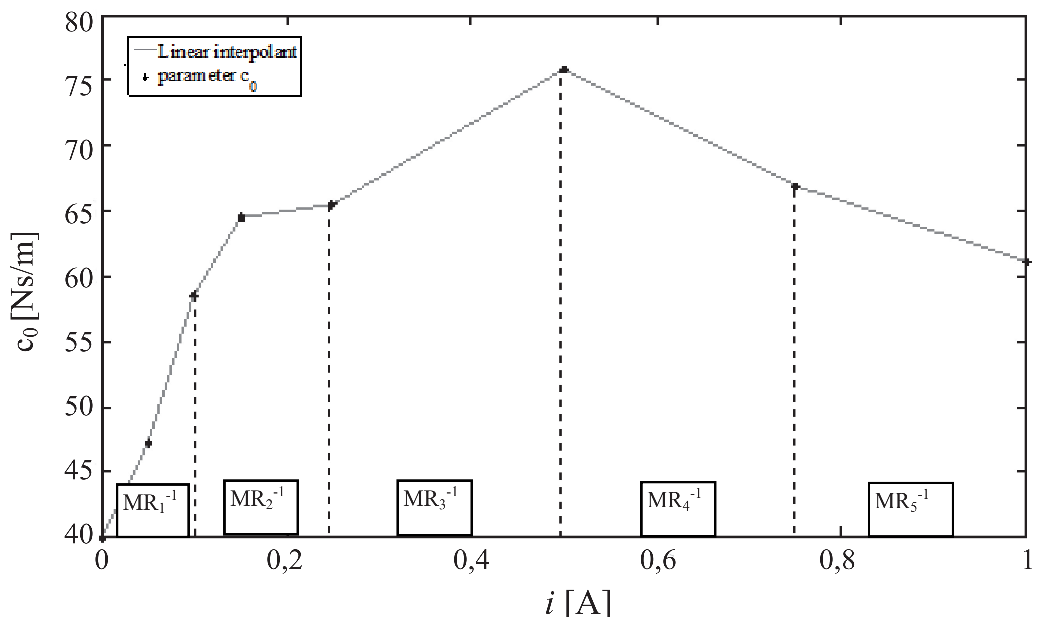

Fig. 4. The c_0 parameter dependence on current i

An inference is proposed to decide, which model should be used for the actual input current i. To reflect operating conditions well, the modelling should be performed for data acquired after the MR damper reaches its operating temperature.

Two complex inverse models, developed for the whole range of operating conditions are presented below for comparison. First inverse model, M_1, is described using (1), where parameters F_c and c_0 are second-degree polynomials dependent on the current. Parameters do not have any physical meaning:

$$\begin{aligned} F_c &= f_{11}i^2 + f_{12}i + f_{13} = -2057i^2 + 3356i + 192 \\ c_0 &= f_{14}i^2 + f_{15}i + f_{16} = -95i^2 + 109i + 45 \end{aligned} \tag{4}$$

M_1 is can be described as follows:

$$i = \frac{-(f_{12}\mathrm{tgh}\left(\beta\left((\dot{x}-\dot{z}) + p_1(x-z)\right)\right) + f_{15}(\dot{x}-\dot{z}) + p_2(x-z)) + \sqrt{\Delta}}{2(f_{11}\mathrm{tgh}\left(\beta\left((\dot{x}-\dot{z}) + p_1(x-z)\right)\right) + f_{14}(\dot{x}-\dot{z}) + p_2(x-z))}, \tag{5}$$

where:

$$\begin{aligned} \Delta = &\{f_{12}\mathrm{tgh}\left(\beta\left((\dot{x}-\dot{z}) + p_1(x-z)\right)\right) + f_{15}(\dot{x}-\dot{z}) + p_2(x-z)\}^2 \\ &-4\{f_{11}\mathrm{tgh}\left(\beta\left((\dot{x}-\dot{z}) + p_1(x-z)\right)\right) + f_{14}(\dot{x}-\dot{z}) + p_2(x-z)\} \cdot \\ &\cdot\{f_{13}\mathrm{tgh}\left(\beta\left((\dot{x}-\dot{z}) + p_1(x-z)\right)\right) + f_{16}(\dot{x}-\dot{z}) + p_2(x-z) - F\} \end{aligned}$$

The second inverse model, M_2, is described using (1), where parameters F_c and c_0 depend on the square root and linear polynomial (Plaza 2008), respectively. Parameters do not have any physical meaning:

$$\begin{aligned} F_c &= f_{21}\sqrt{i} + f_{22} = 1586\sqrt{i} + 79 \\ c_0 &= f_{23}i + f_{24} = 17i + 54 \end{aligned}. \tag{6}$$

M_2 takes the form:

$$i = \left(\frac{-f_{23}(\dot{x}-\dot{z}) + p_2(x-z) + \sqrt{\Delta}}{2f_{21}\mathrm{tgh}\left(\beta\left((\dot{x}-\dot{z}) + p_1(x-z)\right)\right)}\right)^2, \tag{7}$$

where:

$$\begin{aligned} \Delta = &f_{23}(\dot{x}-\dot{z}) + p_2(x-z)^2 - \\ &-4f_{21}\mathrm{tgh}\left(\beta\left((\dot{x}-\dot{z}) + p_1(x-z)\right)\right) \cdot \\ &\cdot\{f_{22}\mathrm{tgh}\left(\beta\left((\dot{x}-\dot{z}) + p_1(x-z)\right)\right) + f_{24}(\dot{x}-\dot{z}) + p_2(x-z) - F_t\} \end{aligned}$$

4. EXPERIMENTS

Simulation experiments have been carried out to verify performance of the control system operating with the cascade of simple models, and results have been compared to those obtained with sophisticated models M_1 and M_2. Performance indices have been defined as follows (Sapiński *et al.* 2003):

$$\begin{aligned} e_1 &= \int_0^T \left(i_e - i_m\right)^2 dt \\ e_2 &= \int_0^T \left(i_e - i_m\right)^2 \left|\frac{dx}{dt}\right| dt \\ e_3 &= \int_0^T \left(i_e - i_m\right)^2 \left|\frac{d\dot{x}}{dt}\right| dt \end{aligned}, \tag{8}$$

where i_e and i_m denote experimental values of the MR damper current, and the simulation value of MR damper model current, respectively. Criteria e_1, e_2, e_3 define the difference between i_e and i_m as functions of time, displacement and velocity, respectively. Obtained results confirm advantages of using a cascade of simple inverse models. Validation scheme is shown in figure 5.

For validation, the current is changed from 0 [A] to 1 [A] with the step of 0.1 [A]. The frequency and amplitude of excitation are constant and set to 2 [Hz] and 25 [mm], respectively. Performance indices are used to compare two inverse models developed for the whole range of operating conditions and the proposed cascade model. Numerical values are shown in figure 6 and collected in table 2.

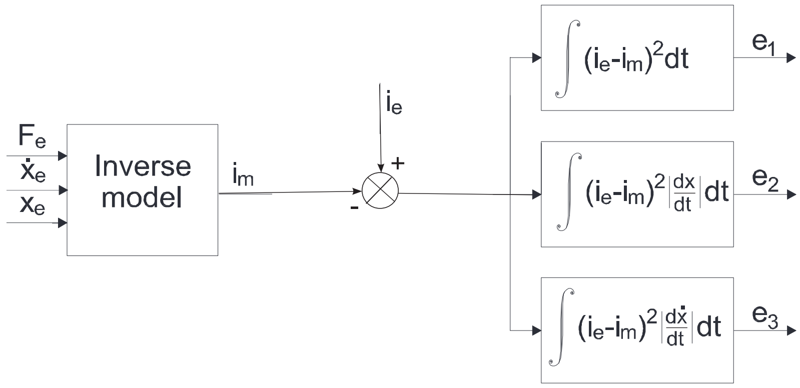

Fig. 5. Validation scheme of the inverse MR damper model

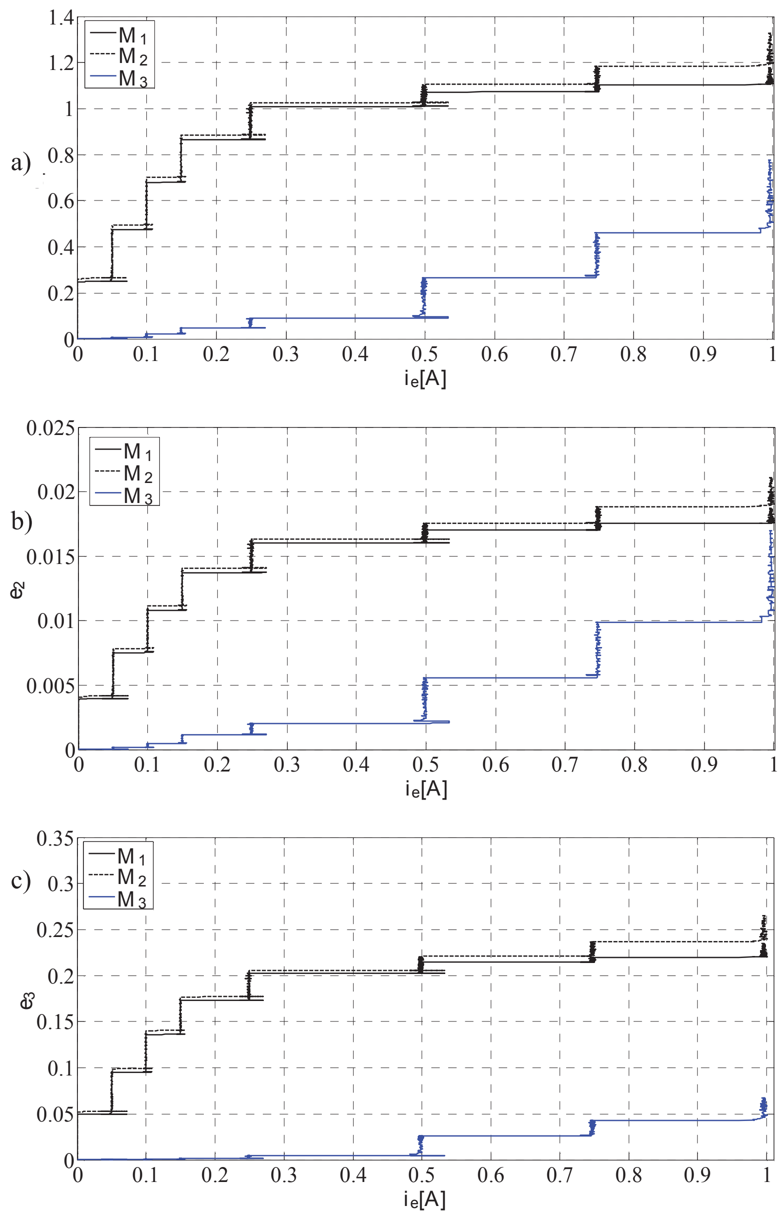

Fig. 6. Time plots of performance indices: a) the difference between i_e and i_m as functions of time, b) the difference between i_e and i_m as functions of displacement, c) the difference between i_e and i_m as functions of velocity

Table 2

Performance indices for all inverse models calculated during validation

Model	e_1	e_2	e_3
M_1	1.266	0.02018	0.2509
M_2	1.485	0.02362	0.2968
M_3	1.090	0.01752	0.0940

Sometimes MR damper does not reach desired force values, because of its dissipative properties. Similar phenomenon occurs for inverse MR damper models.

5. CONCLUSIONS

In the paper, three inverse MR damper models have been compared. Models M_1 and M_2 are those developed for the whole range of operating conditions. In turn, model M_3 is proposed in this paper as a cascade of simple sub-models, each for a different range of the coils current. Three performance indices have been used to validate the proposed approach. It has been shown that it is possible to use a cascade of simple models instead of a complex inverse model. The performance of the cascade model is better than that of complex models. The difference between experimental data and the cascade model data are relatively small for the whole range of operating conditions. The usage of a cascade of simple sub-models guarantees the ability to implement in practice. In case of more complex models its usage can cause additional phase shifting during system operation.

The work reported in this paper has been partially financed by the National Science Centre, decision no. DEC-2011/01/B/ST7/06027. The author would like to thank Mr. T. Machoczek for his help in performing experiments on the material testing system.

References

Bouc R. 1967, *Forced vibration of mechanical systems with hysteresis*. Proceedings of the Fourth Conference on Nonlinear Oscillations, Prague.

Fialho I.J., Balas G.J. 2000, *Design of nonlinear controllers for active vehicle suspensions using parameter-varying control synthesis*. Veh. Syst. Dyn., vol. 33(5), pp. 351–370.

Guo S., Yang S., Pan C. 2006, *Dynamic modelling of magnetorheological damper behaviours*. Journal of Intelligent Material Systems and Structures, vol. 17, no. 1, pp. 3–14.

Kamalakkannan K., Elayaperumal A., Managlaramam S. 2012, *Simulation Aspects of a Full-Car ATV Model Semi Active Suspension*. Engineering, vol. 4, pp. 384–389, DOI 10.4236/eng.2012.47050.

Kurczyk S., Pawełczyk M. 2013, *Fizzy control for semi-active vehicle suspension*. Active Noise and Vibration Control Methods, Krakow–Rytro.

Krauze P. 2011, *Skyhook Control of Front and Rear Magnetorheological Vehicle Suspension*. XIII International PhD Workshop, OWD 2011, pp. 380–385.

Plaza K. 2008, *Modelling and Control for Semi-Active Vibration Damping*. PhD dissertation, Silesian University of Technology.

Sapiński B., Filuś J. 2003, *Analysis of parametric models of MR linear damper*. Journal of Theoretical and Applied Mechanics, vol. 41, pp. 215–240.

Sapiński B. 2009, *Real-Time Control of Magnetorheological Dampers in Mechanical Systems*. AGH Press, Krakow.

Wang D.H., Liao W.H. 2011, *Magnetorheological Fluid Dampers: A Review of Parametric Modelling*. Smart Materials and Structures, vol. 20, pp. 34, DOI 10.1088/0964-1726/20/2/023001

Wolnica M., Pawełczyk M. 2013, *LQR semi-active suspension control for an all-terrain vehicle*. Active Noise and Vibration Control Methods, Kraków–Rytro, pp. 18–19.